ChemComm

COMMUNICATION

View Article Online
View Journal | View Issue



Cite this: *Chem. Commun.*, 2014, **50**, 5031

Received 16th January 2014,
Accepted 21st March 2014

DOI: 10.1039/c4cc00375f

www.rsc.org/chemcomm

# An N-rich metal–organic framework with an *rht* topology: high $CO_2$ and $C_2$ hydrocarbons uptake and selective capture from $CH_4$†

Kang Liu,[a] Baiyan Li,[a] Yi Li,[a] Xu Li,[a] Fen Yang,[a] Guang Zeng,[a] Yu Peng,[a] Zhijuan Zhang,[b] Guanghua Li,[a] Zhan Shi,*[a] Shouhua Feng[a] and Datong Song[c]

**We report the storage capacities and separation selectivity of an *rht*-type *s*-heptazine-based metal organic framework (MOF), $[Cu_3(TDPAH)(H_2O)_3]\cdot 13H_2O\cdot 8DMA$, 1, (where TDPAH is 2,5,8-tris-(3,5-dicarboxylphenylamino)-*s*-heptazine and DMA is *N*,*N*-dimethylacetamide) for $C_2$ hydrocarbons and $CO_2$ over $CH_4$. MOF 1 displays the highest $C_2H_2/CH_4$ selectivity of 80.9 as well as record high $C_2H_4$ and $C_2H_6$ adsorption enthalpies. Theoretical calculations reveal that *s*-heptazine and NH groups within the framework have synergistic effects on $CO_2$ binding.**

Methane, the major component of natural gas, is not only a prevalent and inexpensive fuel for industry and residential use but also a useful $C_1$ feedstock in chemical and petrochemical industries for the production of various $C_1$ and $C_2$ chemicals, such as chloromethanes and acetylene.[1] For chemical and petrochemical applications, impurities in methane as a starting material may complicate the product isolation processes. Moreover, certain impurities may inhibit the conversion of methane. For example, carbon dioxide poisons the Li/MgO catalyst that converts methane into ethane and ethylene.[2] Natural gas contains 80–95% of methane, which requires further purification prior to various chemical processes. The major impurities in naturally occurring methane are $C_2$ hydrocarbons. In addition, carbon dioxide is also present in natural gas in various amounts. It is, therefore, critical to remove carbon dioxide and $C_2$ hydrocarbons from methane. Materials that can preferentially adsorb carbon dioxide and $C_2$ hydrocarbons over methane are highly desirable. Such porous materials can also be used to extract products from the starting material in industrial processes that convert methane into $C_2$ hydrocarbons, such as ethane and acetylene.

Microporous metal–organic frameworks (MOFs) have drawn great attention in recent years[3] and have found use in gas storage and separation, because of their large surface area, tunable pore size and shape, as well as adjustable host–guest interactions. In order to achieve high gas uptake, the *rht*-type MOFs built on supramolecular building blocks (SBBs) serve as an excellent platform. To our knowledge, the first (3,24)-connected *rht*-type MOF was reported by Eddaoudi and co-workers.[4] Thereafter, some remarkable results have been reported (see Fig. S1 and Table S1 in the ESI†). In this family of *rht*-type MOFs, each dendritic hexacarboxylate ligand with 3-fold symmetry is linked by 24 "square paddlewheel" $M_2(COO)_4$ units to form a robust network that possesses both a high concentration of open metal sites (OMSs) and a highly porous structure with a large surface area and pore volume. By adjusting the pore dimensions and functionalizing the interior surface, the gas separation selectivity can be enhanced. Although some progress has been made on porous MOFs for either the adsorption of $C_2$ hydrocarbons[5] and $CO_2$[6] or the separation of $C_2$ hydrocarbons and $CO_2$ over $CH_4$[7,8] at room temperature, MOFs that excel in both tasks are scarce.

Previously, Eddaoudi's group and our group incorporated a 1,3,5-triazine functional group in the ligand structure design for MOF synthesis. The resulting *rht*-type MOF *rht*-MOF-7[9]/Cu-TDPAT[10] (where TDPAT = 2,4,6-tris(3,5-dicarboxylphenylamino)-1,3,5-triazine) exhibited a balance between large storage capacity and high selectivity for $CO_2$. To tune the $CO_2$ affinity, we modified our ligand by replacing the 1,3,5-triazine group with an *s*-heptazine group that has higher density of Lewis basic sites (LBSs). Interestingly, the resulting MOF displays excellent adsorption selectivity for $C_2$ hydrocarbons and $CO_2$ over methane. The preliminary results are reported herein.

Crystals of $[Cu_3(TDPAH)(H_2O)_3]\cdot 13H_2O\cdot 8DMA$, **1**, can be prepared from 2,5,8-tris(3,5-dicarboxylphenylamino)-*s*-heptazine acid ($H_6TDPAH$) and $Cu(NO_3)_2$ under solvothermal conditions in good yield. Single-crystal X-ray diffraction analysis reveals that the three isophthalate moieties in TDPAH are linked through copper paddlewheel units to form cuboctahedral supramolecular building blocks, which are

[a] *State Key Laboratory of Inorganic Synthesis and Preparative Chemistry, College of Chemistry, Jilin University, Changchun 130012, P. R. China. E-mail: zshi@mail.jlu.edu.cn*
[b] *Institute of Atmospheric Environment Safety and Pollution Control, Jinan University, Jinan 510632, P. R. China*
[c] *Davenport Chemical Research Laboratories, Department of Chemistry, University of Toronto, 80 St. George Street, Toronto, Ontario, Canada*

† Electronic supplementary information (ESI) available: Experimental details and characterization data, as well as CIF files. CCDC 928821. For ESI and crystallographic data in CIF or other electronic format see DOI: 10.1039/c4cc00375f

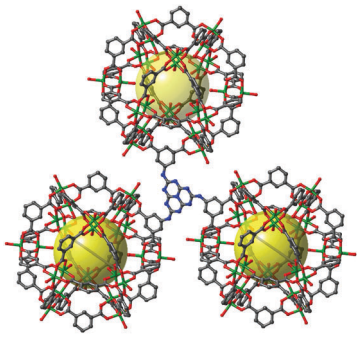

Fig. 1 Structure of **1**. A portion of the (3,24)-connected *rht*-net built on TDPAH is shown (Cu, green; C, gray; O, red; N, blue. H atoms are omitted for clarity).

covalently bonded through the isophthalate moieties to yield a (3,24)-connected *rht*-type network of **1** (Fig. 1). Similar to other reported (3,24)-connected structures, such as PCN-61, NU-100, NOTT-112 and Cu-TPBTM, there are three types of cages, namely, cuboctahedron (cub-$O_h$), truncated tetrahedron (T-$T_d$), and truncated octahedron (T-$O_h$) in **1** in a 1 : 2 : 1 ratio (see Fig. S4 in the ESI†). The diameters of spheres representing the void inside these polyhedra are 1.2, 1.04 and 1.72 nm, respectively. The total accessible volume after the removal of the guest and coordinated solvent molecules is 71.7% using the PLATON/VOID routine,[11] and the calculated density of the desolvated framework is 0.775 g cm$^{-3}$.

The activated samples were prepared by exchanging the solvent in the as-synthesized **1** with $CH_3OH$, followed by evacuation under high vacuum at 100 °C for 10 h. A comparison of PXRD patterns of as-synthesized, activated **1** and **1** after adsorption of $CO_2$ was made carefully. The water/moisture stability was tested in boiling water (1 day) and in air (30 days). The framework remained intact as clearly indicated by the PXRD patterns of the samples recorded after these tests (see Fig. S6 and S7 in the ESI†). Permanent porosity of activated **1** was confirmed by $N_2$ adsorption–desorption isotherms at 77 K which showed a reversible type-I isotherm (see Fig. S9 and S10 in the ESI†). The Langmuir and BET surface areas are 2540 and 2171 m$^2$ g$^{-1}$, respectively. The total pore volume calculated from the $N_2$ isotherms is 0.91 cm$^3$ g$^{-1}$, which is in good agreement with the value calculated from single-crystal data which is 0.89 cm$^3$ g$^{-1}$.

The $CO_2$ low-pressure adsorption–desorption isotherms of **1** were measured at 273, 288, and 298 K (0–1 atm). At 298 K, the uptake amounts are 116 cm$^3$ g$^{-1}$ (STP = standard temperature and pressure; 22.8 wt%, 90 v/v) and 20.2 cm$^3$ g$^{-1}$ (STP; 4.0 wt%, 16 v/v) at 1.0 and 0.1 atm, respectively. At 273 K, they are 192 cm$^3$ g$^{-1}$ (STP; 37.7 wt%, 149 v/v) and 50.6 cm$^3$ g$^{-1}$ (STP; 9.9 wt%, 39 v/v) at 1.0 and 0.1 atm, respectively (see Fig. 2a and Fig. S13 in the ESI†). These values are substantially higher than those obtained for most of the previously reported *rht*-type structures (Table S3 in ESI†), and among the highest for MOFs reported to date with both OMSs and LBSs (Table S4 in ESI†). To the best of our knowledge, the LBS density is the highest (5.4 nm$^{-3}$) in *rht*-MOFs. Compared with $CO_2$, $N_2$ and $CH_4$ were hardly adsorbed at 273 K and 298 K. From these data, the calculated $CO_2/N_2$ and $CO_2/CH_4$ adsorption selectivities based on Henry's law selectivity are 69.3 : 1 and 20.3 : 1 at 273 K and 36.7 : 1 and 10.0 : 1 at 298 K, respectively. At 298 K and 48 bar, the excess $CO_2$ uptakes of **1** reach 17.1 mmol g$^{-1}$. Its volumetric capacity is 297 v/v. Detailed information is provided in the ESI† (Fig. S40).

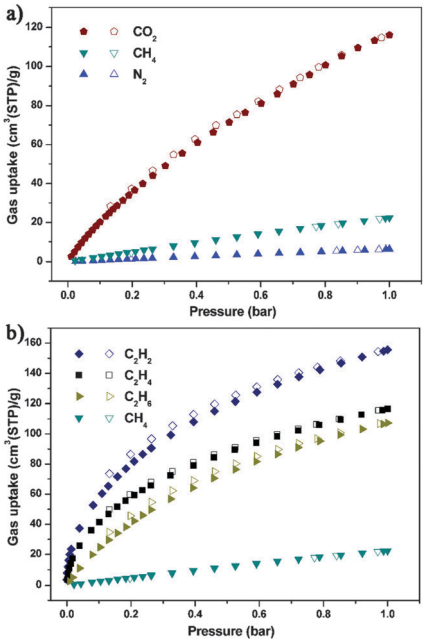


Fig. 2 (a) $CO_2$, $CH_4$ and $N_2$ sorption isotherms at 298 K (adsorption: filled; desorption: open). (b) $C_2H_2$, $C_2H_4$, $C_2H_6$ and $CH_4$ sorption isotherms at 298 K. (adsorption: filled; desorption: open).

The $C_2$ hydrocarbons ($C_2H_2$, $C_2H_4$ and $C_2H_6$) and $C_1$ ($CH_4$) hydrocarbon low-pressure adsorption–desorption isotherms of **1** were measured at 273 and 298 K (0–1 atm). The uptake capacities at 1 atm and 273 K for $C_2H_2$, $C_2H_4$, $C_2H_6$, and $CH_4$ are 202.2, 163.9, 162.9, and 32.7 cm$^3$ g$^{-1}$, respectively, while those at 1 atm and 298 K are 155.7, 116.7, 107.2, and 22.4 cm$^3$ g$^{-1}$, respectively. (see Fig. 2b, Fig. S16, S19, S22 and S25 in the ESI†). The uptake capacity of **1** for $C_2H_2$ at 298 K is among the highest for MOF materials (*e.g.* HKUST (201 cm$^3$ g$^{-1}$), CoMOF-74 (197 cm$^3$ g$^{-1}$), NOTT-101 (184 cm$^3$ g$^{-1}$), PCN-16 (176 cm$^3$ g$^{-1}$), $Cu_2$(ebtc) (160 cm$^3$ g$^{-1}$) and UTSA-20 (150 cm$^3$ g$^{-1}$)). The separation ratios of $C_2$ hydrocarbons ($C_2H_2$, $C_2H_4$ and $C_2H_6$) *versus* $C_1$($CH_4$) are based on Henry's law selectivity. The calculated $C_2H_2/CH_4$, $C_2H_4/CH_4$ and $C_2H_6/CH_4$ adsorption selectivities at 273 K are 102.3 : 1, 75.4 : 1, and 27.1 : 1, respectively, while those at 298 K are 80.9, 40.6 : 1, and 12.5 : 1, respectively (some virial parameters are summarized in Table S6, ESI†). To the best of our knowledge, the $C_2H_2/CH_4$ separation selectivity of 80.9 is the highest to date (see Table S5 in the ESI†).

The isosteric heats ($Q_{st}$) of **1** for the five gases ($CO_2$, $CH_4$, $C_2H_2$, $C_2H_4$, and $C_2H_6$) were calculated using the virial method,[12] which is a well-established and reliable methodology fitting from their adsorption isotherms at 273 and 298 K (273, 288, and 298 K for $CO_2$). The low coverage $Q_{st}$ value of $CO_2$ adsorption in **1** (33.8 kJ mol$^{-1}$) is the second highest one among values of the reported *rht*-MOFs, while Cu-TDPAT exhibits the highest value (42.2 kJ mol$^{-1}$) so far. The isosteric heats at zero coverage are 33.0, 45.0, 23.5 and 13.8 kJ mol$^{-1}$ for $C_2H_6$, $C_2H_4$, $C_2H_2$ and $CH_4$, respectively. It is worth noting that compound **1** shows the highest adsorption enthalpy of $C_2H_6$ (33.0 kJ mol$^{-1}$) and $C_2H_4$ (45 kJ mol$^{-1}$) at zero loading for MOFs under the same

 

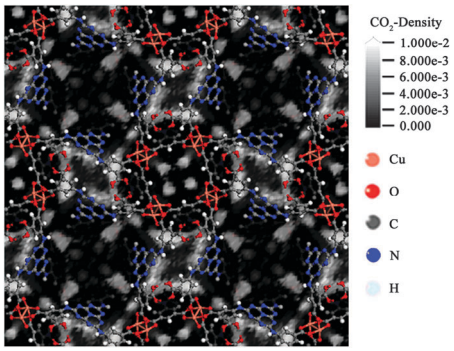


Fig. 3 Density distribution of the center-of-mass of $CO_2$ molecules along the *c*-axis in the unit cell of **1** at 273 K and 1 bar simulated by GCMC.

conditions.[13] The adsorption enthalpies for $CO_2$, $C_2H_2$, $C_2H_4$ and $C_2H_6$ are all greater than that for $CH_4$, presumably because of the combined effects of the van der Waals host–guest interactions and the electrostatic host–guest interactions in this system, thus leading to high selectivity for $C_2$ hydrocarbons and $CO_2$ over $CH_4$. (see Fig. S13–S27 in the ESI†).

To imitate the separation behaviour of **1** under a more real-world setting, the gas selectivities ($CO_2/CH_4$, $C_2H_2/CH_4$, $C_2H_4/CH_4$ and $C_2H_6/CH_4$) in a binary mixture were calculated employing the ideal adsorbed solution theory (IAST) method[14] with the experimental single-component isotherms fitted by the dual-site Langmuir (DSL) model.[15] (see Table S9 in the ESI†). The selectivities of $C_2$ components ($C_2H_2$, $C_2H_4$, and $C_2H_6$) and $CO_2$ with respect to $CH_4$ are in excess of 82, 54, 24 and 18, respectively, for a range of pressures up to 100 kPa (see Fig. S44 in the ESI†).

To probe the nature of $CO_2$ adsorption at the molecular level, GCMC and first-principles calculations were carried out. The density distribution of the center-of-mass of $CO_2$ molecules obtained from GCMC simulations reveals that $CO_2$ molecules in **1** prefer to locate at both the open $Cu^{II}$ metal sites and NH groups within the framework (see Fig. 3 and Fig. S43 in the ESI†). In order to investigate the role of the *s*-heptazine groups, we calculated the binding energies of $CO_2$ at NH sites using the first-principles method in three model compounds: (a) with three NH groups on an *s*-heptazine core, (b) replacing the six peripheral nitrogen atoms of the *s*-heptazine core in (a) with carbon atoms, and (c) replacing the central nitrogen atom of (b) with a carbon atom (see Fig. 4). The $CO_2$ binding energy of the NH site in (a) is up to $-10.30$ kJ mol$^{-1}$, while those in (b) and (c) are both $-4.07$ kJ mol$^{-1}$. We attribute this difference to the polarization of $CO_2$ molecules by the adjacent nitrogen lone pairs on the *s*-heptazine group, which displays the synergistic effects with NH–$CO_2$ interactions in (a) to enhance the $CO_2$ affinity.

In summary, we prepared and structurally characterized a highly porous *rht*-MOF, **1**, which exhibits high adsorption capability for $C_2$ hydrocarbons and $CO_2$ with excellent selectivity for $C_2$ hydrocarbons and $CO_2$ over $CH_4$ as well as record high $C_2H_4$ and $C_2H_6$ adsorption enthalpies. Theoretical calculations indicate that *s*-heptazine and NH groups within the framework

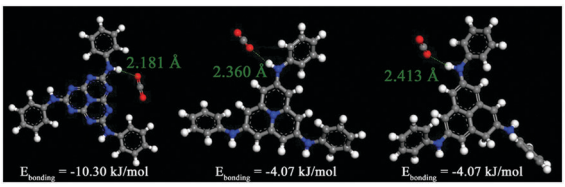


Fig. 4 Preferential $CO_2$ adsorption sites and the corresponding binding energies obtained from first-principles calculations.

have synergistic effects on $CO_2$ binding. The selective adsorption properties of **1** make it a promising candidate for methane purification and recycling. Future efforts in our laboratory will focus on the frameworks with an imino *s*-heptazine backbone to further improve the $C_2$ and $CO_2$ storage capacity and selectivity. We found a newly published study by Eddaoudi group reporting similar results during the proof stage.[16]

This work was financially supported by the Foundation of the National Natural Science Foundation of China (No. 21371069).

## Notes and references

1 A. U. Czaja, N. Trukhanb and U. Müller, *Chem. Soc. Rev.*, 2009, **38**, 1284–1293.
2 S. Al-Zahrani, Q. Song and L. L. Lobban, *Ind. Eng. Chem. Res.*, 1994, **33**, 251–258.
3 (*a*) J. Lee, O. K. Farha, J. Roberts, K. A. Scheidt, S. T. Nguyen and J. T. Hupp, *Chem. Soc. Rev.*, 2009, **38**, 1450–1459; (*b*) M. P. Suh, H. J. Park, T. K. Prasad and D. W. Lim, *Chem. Rev.*, 2012, **112**, 782–835; (*c*) S. Ma and H. C. Zhou, *Chem. Commun.*, 2010, **46**, 44–53.
4 F. Nouar, J. F. Eubank, T. Bousquet, L. Wojtas, M. J. Zaworotko and M. Eddaoudi, *J. Am. Chem. Soc.*, 2008, **130**, 1833–1835.
5 (*a*) S. Xiang, W. Zhou, J. M. Gallegos, Y. Liu and B. Chen, *J. Am. Chem. Soc.*, 2009, **131**, 12415–12419; (*b*) S. Xiang, W. Zhou, Z. Zhang, M. A. Green, Y. Liu and B. Chen, *Angew. Chem.*, 2010, **122**, 4719–4722 (*Angew. Chem., Int. Ed.*, 2010, **49**, 4615–4618).
6 (*a*) K. Sumida, D. L. Rogow, J. A. Mason, T. M. McDonald, E. D. Bloch, Z. R. Herm, T. H. Bae and J. R. Long, *Chem. Rev.*, 2012, **112**, 724–781; (*b*) Q. Wang, J. Luo, Z. Zhong and A. Borgna, *Energy Environ. Sci.*, 2011, **4**, 42–55.
7 (*a*) Y. He, W. Zhou, R. Krishna and B. Chen, *Chem. Commun.*, 2012, **48**, 11813–11831; (*b*) H. Wu, Q. Gong, D. H. Olson and J. Li, *Chem. Rev.*, 2012, **112**, 836–868; (*c*) J. R. Li, J. Sculley and H. C. Zhou, *Chem. Rev.*, 2012, **112**, 869–932.
8 (*a*) S. Horike, Y. Inubushi, T. Hori, T. Fukushima and S. Kitagawa, *Chem. Sci.*, 2012, **3**, 116–120; (*b*) S. Couck, J. F. M. Denayer, G. V. Baron, T. Remy, J. Gascon and F. Kapteijn, *J. Am. Chem. Soc.*, 2009, **131**, 6326–6327; (*c*) D. Britt, H. Furukawa, B. Wang, T. G. Glover and O. M. Yaghi, *Proc. Natl. Acad. Sci. U. S. A.*, 2009, **106**, 20637–20640.
9 R. Luebke, J. F. Eubank, A. J. Cairns, Y. Belmabkhout, L. Wojtas and M. Eddaoudi, *Chem. Commun.*, 2012, **48**, 1455–1457.
10 B. Li, Z. Zhang, Y. Li, K. Yao, Y. Zhu, Z. Deng, F. Yang, X. Zhou, G. Li, H. Wu, N. Nijem, Y. J. Chabal, Z. Lai, Y. Han, Z. Shi, S. Feng and J. Li, *Angew. Chem.*, 2012, **124**, 1441–1444 (*Angew. Chem., Int. Ed.*, 2012, **51**, 1412–1415).
11 A. L. Spek, *PLATON: A Multipurpose Crystallographic Tool*, Utrecht University, Utrecht, The Netherlands, 2001.
12 J. L. C. Rowsell and O. M. Yaghi, *J. Am. Chem. Soc.*, 2006, **128**, 1304–1315.
13 E. D. Bloch, W. L. Queen, R. Krishna, J. M. Zadrozny, C. M. Brown and J. R. Long, *Science*, 2012, **335**, 1606–1610.
14 Y. S. Bae, O. K. Farha, A. M. Spokoyny, C. A. Mirkin, J. T. Hupp and R. Q. Snurr, *Chem. Commun.*, 2008, 4135–4137.
15 (*a*) S. Keskin, J. Liu, J. K. Johnson and D. S. Sholl, *Langmuir*, 2008, **24**, 8254–8261; (*b*) S. Keskin, J. Liu, R. B. Rankin, J. K. Johnson and D. S. Sholl, *Ind. Eng. Chem. Res.*, 2009, **48**, 2355–2371.
16 R. Luebke, Ł. J. Weseliński, Y. Belmabkhout, Z. Chen, Ł. Wojtas and M. Eddaoudi, *Cryst. Growth Des.*, 2014, **14**, 414–418.